15. Ho, D. D. *et al.* Rapid turnover of plasma virions and CD4 lymphocytes in HIV-1 infection. *Nature* **373,** 123–126 (1995).
16. Wei, X. *et al.* Viral dynamics in human immunodeficiency virus type 1 infection. *Nature* **373,** 117–122 (1995).
17. Perelson, A. S., Neumann, A. U., Markowitz, M., Leonard, J. M. & Ho, D. D. HIV-1 dynamics *in vivo*: virion clearance rate, infected cell life-span, viral generation time. *Science* **271,** 1582–1586 (1986).
18. Coffin, J. M. HIV population dynamics *in vivo*: Implications for genetic variation, pathogenesis, and therapy. *Science* **267,** 483–489 (1995).
19. Zack, J. A. *et al.* HIV-1 entry into quiescent primary lymphocytes: molecular analysis reveals a labile, latent viral structure. *Cell* **61,** 213–222 (1990).
20. Bukrinsky, M. I. *et al.* Active nuclear import of human immunodeficiency virus type 1 preintegration complexes. *Proc. Natl Acad. Sci. USA* **89,** 6580–6584 (1992).
21. Chun, T.-W. *et al.* Fate of HIV-1-infected T cells *in vivo*: Rates of transition to stable latency. *Nature Med.* **1,** 1284–1290 (1995).
22. Pauza, C. D. Two bases are deleted from the termini of HIV-1 linear DNA during integrative recombination. *Virology* **179,** 886–889 (1990).
23. Brown, P. O., Bowerman, B., Varmus, H. E. & Bishop, J. M. Retroviral integration: Structure of the initial covalent product and its precursor, and a role for the viral IN protein. *Proc. Natl Acad. Sci. USA* **86,** 2525–2529 (1989).
24. Dimitrov, D. S. *et al.* Quantitation of human immunodeficiency virus type 1 infection kinetics. *J. Virol.* **67,** 2182–2190 (1993).
25. Gartner, S. *et al.* The role of mononuclear phagocytes in HTLV-III/LAV infection. *Science* **233,** 215–219 (1986).
26. Dickover, R. E. *et al.* Decreases in unintegrated HIV DNA are associated with antiretroviral therapy in AIDS patients. *J. Acq. Imm. Def. Syndr.* **5,** 31–36 (1992).
27. Michie, C. A., McLean, A., Alcock, C. & Beverley, P. C. Lifespan of human lymphocyte subsets defined by CD45 isoforms. *Nature* **360,** 264–265 (1992).
28. Patel, S. S., Duby, A. D., Tiele, D. L. & Lipsky, P. E. Phenotypic and functional characterization of human T cell clones. *J. Immunol.* **141,** 3726–3736 (1988).
29. Myers, L. A., McQuay, L. J. & Hollinger, F. B. Dilution assay statistics. *J. Clin. Microbiol.* **32,** 732–739 (1994).
30. Perelson, A. S. *et al.* Decay characteristics of HIV-1-infected compartments during combination therapy. *Nature* **387,** 188–191 (1997).

Supplementary information is available on *Nature's* World-Wide Web site (http://www.nature.com) or as paper copy from Mary Sheehan at the London editorial office of *Nature*.

Acknowledgements. We thank E. Cornell for coordinating clinical aspects of the study, P. Lietman, J. Boeke, R. Markum and M. Schlissel for discussion and A. Siliciano for editorial assistance. This study was supported by the NIH and by the Johns Hopkins Outpatient General Clinical Research Center.

Correspondence and requests for materials should be addressed to R.F.S. (e-mail: rsilicia@welchlink.welch.jhu.edu).

Decay characteristics of HIV-1-infected compartments during combination therapy

Alan S. Perelson, Paulina Essunger, Yunzhen Cao*, Mika Vesanen*, Arlene Hurley*, Kalle Saksela†, Martin Markowitz* & David D. Ho*

Theoretical Division, Los Alamos National Laboratory, Los Alamos, New Mexico 87545, USA
** Aaron Diamond AIDS Research Center, The Rockefeller University, 455 First Avenue, New York, New York 10016, USA*
† Institute of Medical Technology, University of Tampere, Tampere, Finland

Analysis of changes in viral load after initiation of treatment with potent antiretroviral agents has provided substantial insight into the dynamics of human immunodeficiency virus type 1 (HIV-1)[1–3]. The concentration of HIV-1 in plasma drops by ~99% in the first two weeks of treatment owing to the rapid elimination of free virus with a half-life ($t_{1/2}$) of ≤6 hours and loss of productively infected cells with a $t_{1/2}$ of 1.6 days[3]. Here we show that with combination therapy this initial decrease is followed by a slower second-phase decay of plasma viraemia. Detailed mathematical analysis shows that the loss of long-lived infected cells ($t_{1/2}$ of 1–4 weeks) is a major contributor to the second phase, whereas the activation of latently infected lymphocytes ($t_{1/2}$ of 0.5–2 weeks) is only a minor source. Based on these decay characteristics, we estimate that 2.3–3.1 years of a completely inhibitory treatment would be required to eliminate HIV-1 from these compartments. To eradicate HIV-1 completely, even longer treatment may be needed because of the possible existence of undetected viral compartments or sanctuary sites.

Eight HIV-1-infected patients were studied who were naive to antiretroviral agents, with baseline CD4 lymphocyte counts ranging from 26 to 505 per μl (Table 1). *De novo* HIV-1 replication in the patients was blocked by the combined use of a protease inhibitor, nelfinavir[4] (2,250 mg d^{-1}), and two reverse transcriptase inhibitors, zidovudine (600 mg d^{-1}) and lamivudine (300 mg d^{-1}). After treatment was started, the HIV-1 RNA concentration in plasma was measured weekly for the first month and then every two weeks using the branched DNA (bDNA) assay[2,3]. Each patient responded with a similar pattern of viral decay (Fig. 1): an initial rapid exponential decline of nearly 2-logs (first phase), consistent with previous observations[1–3], followed by a slower exponential decline (second phase). The antiretroviral effect was potent in that plasma viraemia in all eight patients dropped below the standard detection threshold of 500 copies ml^{-1} by 8 weeks of treatment, and was found to be <25 copies ml^{-1} at week 16–20 by using an ultra-sensitive modification of the bDNA assay (data not shown). In addition, no infectious HIV-1 was detectable in 10^7 peripheral blood mononuclear cells (PBMC) from each of the patients after 8 weeks of treatment. These findings not only attest to the potency of the antiretroviral regimen, but also to the lack of emergence of drug-resistant virus during the study period.

The second phase in the decay profile is probably due to sources of HIV-1 not included in our previous analysis[3], such as infected tissue macrophages or dendritic cells, activation of latently infected lymphocytes, or release of trapped virions[2,3,5,6]. If such 'secondary' sources are initially responsible for, say, 1% of the virions in plasma, then the rapid decline in viraemia would slow when the productively infected $CD4^+$ T cells, T^*, had decayed to about 1% of their initial level. Further decay of T^* at their fast $t_{1/2}$ would then leave the secondary sources as the major producers of virions. The slower decay of the major secondary source would then be reflected in the slope of the second-phase decline.

Here we incorporate secondary sources of virus into a new model and analyse data obtained from the patients. The model contains cells, M, which upon infection with a rate constant, k_M, become long-lived infected cells, M^*, which produce virus continuously at an average rate per cell, p, and are lost with a rate constant μ_M. We also assume that when $CD4^+$ T cells, T, are infected, T^* cells are generated with a rate constant k and that latently infected T cells containing infectious provirus are generated with a rate constant fk, smaller by a factor f. Latently infected lymphocytes, L, are assumed to die with a rate constant δ_L, and to be activated into productively infected cells with rate constant a, giving a total rate constant of loss $\mu_L = a + \delta_L$. T^* are lost with a rate constant, δ, and are assumed to produce a total of N virions (the burst size) during their lifetime. Virions, V, are cleared with a rate constant c. Thus, as a new kinetic model, we propose: $dT^*/dt = kVT + aL - \delta T^*$; $dL/dt = fkVT - \mu_L L$; $dM^*/dt = k_M VM - \mu_M M^*$ and $dV/dt = N\delta T^* + pM^* - cV$.

Virions are produced by infected cells in both tissues and blood, although most such cells will be in tissues[7]. Using methods similar to those already published[3], assuming that both HIV-1 reverse transcriptase and protease are completely inhibited by the antiretroviral regimen and that the system was at steady-state before treatment, with baseline viral load V_0 and $CD4^+$ T-cell count T_0, the level of plasma virus after drug therapy should decay as follows:

$$V(t) = V_0[Ae^{-\delta t} + Be^{-\mu_L t} + Ce^{-\mu_M t} + (1 - A - B - C)e^{-ct}] \quad (1)$$

where

$$A = \frac{NkT_0}{c - \delta}\left(1 - \frac{af}{\delta - \mu_L}\right)$$

$$B = \frac{af\delta NkT_0}{\mu_L(\delta - \mu_L)(c - \mu_L)}$$

$$C = \frac{c - NkT_0\left(1 + \frac{af}{\mu_L}\right)}{c - \mu_M}$$

Here pharmacokinetic and intracellular delays[8] are ignored as we are interested in effects that occur on a timescale of weeks to months. If the drugs are not completely inhibitory, then the model needs to be supplemented by equations for the uninfected populations T and M. When $f = 0$, no latently infected T cells are generated and this solution reduces to one for a model with the second phase being generated solely by long-lived cells. We call this the long-lived infected cell model.

We observed, down to the HIV-1 RNA detection limit, only two phases in the viral decay curves of each of the eight patients. This suggests that in each patient there is only one major secondary source of virions. Fitting the plasma viraemia data with the long-lived infected cell model, using nonlinear least-squares regression, we estimate the parameters δ, μ_M, and a composite parameter, NkT_0. Virion clearance occurs too rapidly to estimate c from the available data in this study. Thus, c was held constant at the mean value, $c = 3\,d^{-1}$, determined previously[3]. Three examples of the best-fit curves generated from equation (1), with $f = 0$, are shown in Fig. 1.

The equation for $V(t)$ can also be reduced to the solution of a model with only latently infected T cells instead of long-lived cells. Fitting the plasma viraemia data with this latently-infected cell model gave fits that were indistinguishable from that of the long-lived

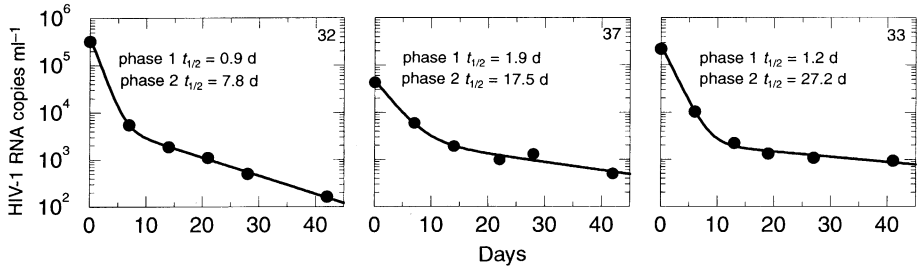

Figure 1 Plasma levels of HIV-1 RNA (filled circles) measured by the bDNA assay for three representative patients during triple therapy, begun on day 0; data points between 100 and 500 copies ml^{-1} were determined using 10 ml plasma. The theoretical curve (solid line) was obtained by nonlinear least-square fitting of the logarithm of equation (1), with $f = 0$, to the logarithm of the data. The parameters δ, μ_M and NkT_0, were simultaneously estimated. The parameter estimates obtained were: patient 32, see Table 1; patient 33, $\delta = 0.57\,d^{-1}$, $\mu_M = 0.025\,d^{-1}$, and $NkT_0 = 2.97$; patient 37, $\delta = 0.36\,d^{-1}$, $\mu_M = 0.040\,d^{-1}$, and $NkT_0 = 2.80$.

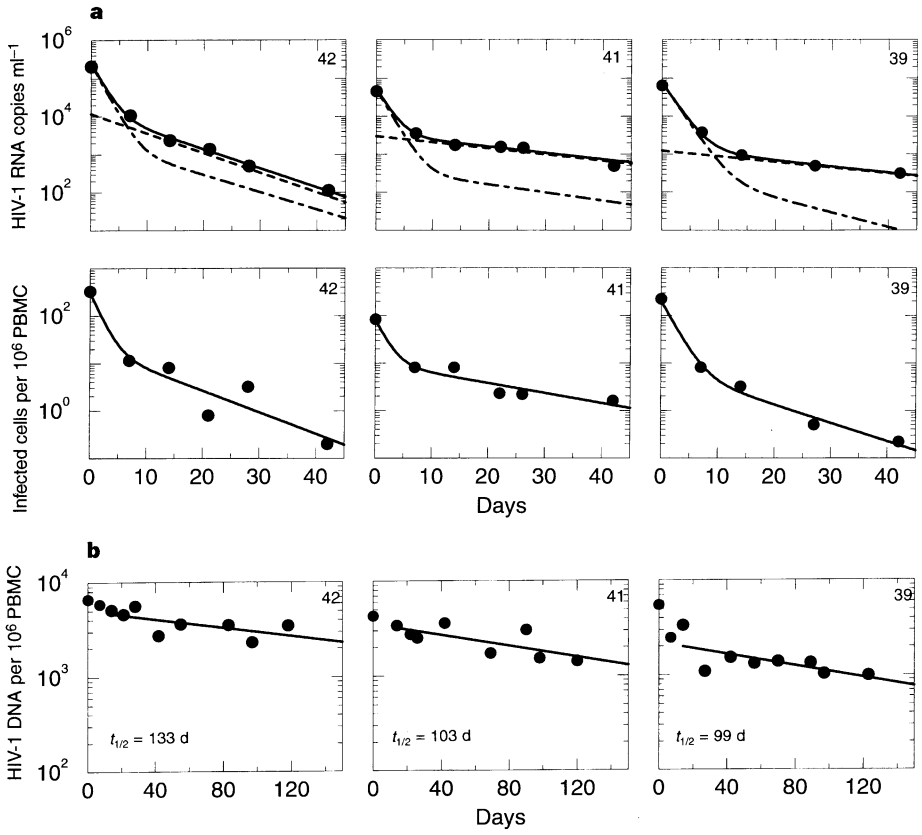

Figure 2 **a**, Plasma levels of HIV-1 RNA, PBMC infectivity, and **b**, HIV-1 proviral DNA for three representative patients. The theoretical curves (solid lines) were obtained by fitting equations (1) and (2) simultaneously to the data (filled circles). The long-dashed short-dashed line indicates the contribution to the total HIV-1 RNA by pre-existing productively infected T cells plus those generated by the gradual activation of latently infected T cells (the terms $Ae^{-\delta t} + Be^{-\mu_L t}$ in equation (1)); the dashed line indicates the contribution made by long-lived infected cells, M^* (the term $Ce^{-\mu_M t}$ in equation (1)). By day 14, the productively infected $CD4^+$ T cells initially present have substantially decayed, and the remaining productively infected T cells are being generated by activation of laterally infected T cells. As indicated by the long-dashed short-dashed line after day 14, the contribution to the second phase made by latently infected T cells is substantially smaller than the contribution made by long-lived infected cells (dashed line).

infected cell model for each of the eight patients. Thus, additional viral-load data were obtained in order to distinguish between the models. At each time point, the infectivity titre of HIV-1 in PBMC was measured by limiting dilution (5-fold serially; quadruplicate samples), as described[9,10]. The number of infected cells per 10^6 PBMC was estimated using maximum likelihood[11]. In patient 40, infectivity dropped to below the detection threshold too rapidly to permit a detailed analysis. Patient 32 has a plasma viral load that was not in steady state before treatment and therefore could not be analysed further.

In the PBMC infectivity assays, cells that latently harbour infectious provirus would be activated *in vitro* and thus would be scored in the limiting-dilution measurement. If we assume that long-lived, virus-producing cells reside in tissues and that the number of infected $CD4^+$ T cells in blood are proportional to the total number in the body, then the number of PBMC carrying infectious HIV-1 detected in the PBMC infectivity assay is proportional to $I(t) = T^*(t) + L(t)$, where

$$I(t) = \frac{kV_0T_0}{\delta}\left[\left(1 - \frac{af}{\delta - \mu_L}\right)e^{-\delta t} + \frac{f\delta}{\mu_L}\left(1 + \frac{a}{\delta - \mu_L}\right)e^{-\mu_L t}\right] \quad (2)$$

Simultaneously fitting equations (1) and (2) to the plasma viraemia and PBMC infectivity data yielded estimates of the various decay rate constants (Table 1). In general, 10–12 data points were used in the fitting, with an average of 6.4 data points specifically during the second phase (see Fig. 2a for examples). The parameter, μ_M, for long-lived infected cells ranged from 0.028 to 0.119 d^{-1}, with a mean value of 0.061 ± 0.033 d^{-1}. The corresponding half-life, $t_{1/2} = \ln 2/\mu_M$, had a mean value of 14.1 ± 7.5 d, and was negatively correlated with the logarithm of the baseline viral load ($r^2 = 0.77$, $p < 0.03$). The parameter, δ, for productively infected T cells ranged from 0.36 to 1.2 d^{-1}, with a mean of 0.69 ± 0.25 d^{-1}. The corresponding $t_{1/2}$ values ranged from 0.6 to 1.9 d, with a mean of 1.1 ± 0.4 d. The parameter, μ_L, for cells latently carrying infectious provirus ranged from 0.049 to 0.181 d^{-1}, with a mean of 0.098 ± 0.048 d^{-1}. The corresponding $t_{1/2}$ ranged from 3.8 to 14.1 d, with a mean of 8.5 ± 4.0 d. As $c = 3\,d^{-1}$ was a minimal estimate[3], we also examined the effect of using $c = 30\,d^{-1}$. This led to minor changes in our parameter estimates (<10% for δ, <5% for μ_M and μ_L).

Most infected PBMC harbour defective provirus[1,12] and cannot be activated into virus production. We measured the rate of decay of PBMC proviral DNA, δ_{DNA}, by a standard method[13]. In several patients, the DNA data suggested a more rapid first phase, possibly due to the loss of transiently and productively infected cells. Here we are concerned with the turnover of stably infected cells and only analyse the data from day 14 onwards. As shown in Fig. 2b and Table 1, δ_{DNA} ranged between 0.0016 and 0.033 d^{-1}, with a mean of 0.012 ± 0.011 d^{-1}. The corresponding $t_{1/2}$ values ranged from 21 to 433 d, with a mean of 145 d, which is somewhat longer than previous estimates[1,12], but similar to the $t_{1/2}$ of $CD4^+$ $CD45RO^+$ T cells[14]. The rate of proviral decay was therefore substantially slower than that of plasma viraemia or PBMC infectivity decay, suggesting that this DNA is mainly harboured within cells that contain proviruses that cannot be activated to produce infectious virus. While latently infected T cells are a subset of the provirus-containing cells, we chose to estimate δ_L by δ_{DNA}, because in fitting equations (1) and (2), we could not separately determine the loss parameters a and δ_L. Changing δ_L tenfold led only to minor changes (<10%) in the $t_{1/2}$ estimates shown in Table 1.

Table 2 Length of treatment (yr) to eradicate HIV-1 from long-lived cells

Second phase half-life	Initial number of infected long-lived cells: 10^9	10^{12}
1 week	0.6	0.8
2 weeks	1.2	1.5
4 weeks	2.3	3.1

From the parameter estimates and equation (1) for $V(t)$, we can compute the contribution of latently infected T cells and long-lived cells to the viral load. As shown in Fig. 2a, long-lived infected cells are the major contributor of virions to the second phase of plasma viraemia decay. Furthermore, at the pretreatment steady state, the fraction of plasma virions produced by long-lived infected cells ranged from 1 to 7% (Table 1), whereas the contribution by activation of latently infected T cells was ≤1% (Fig. 2a). Thus, 93–99% of the plasma viraemia at steady state was sustained by productively infected T cells, as we reported previously[3]. From the steady-state conditions and parameter values in Table 1, we computed that the ratio T_0^*/L_0 had a mean of 15.9 ± 11.3, which is similar to the value previously reported[15,16]. Latently infected T cells with stably integrated DNA may arise from productively infected $CD4^+$ T cells reverting to a resting state[16]. Modifying our model so that L arises from T^* rather than from T, we find little difference in our estimate of $t_{1/2}$ for latently infected T cells or T_0^*/L_0 (data not shown).

We find that the principal contributor to the second phase of plasma viral decay has a $t_{1/2}$ of 5.8 to 24.8 d (Table 1). Based on experimental observations that some tissue macrophages are infected *in vivo*[17–19] and that macrophages infected *in vitro* can continuously release virions for weeks[20,21], the long-lived population defined here may consist of tissue macrophages. Theoretically, virions trapped on follicular dendritic cells in lymphoid tissues

Table 1 Summary of infected-cell-loss rates for eight patients

Parameter estimates from fit of $V(t)$ to plasma viral load and $I(t)$ to cell infectivity data

Patient	Baseline values		Infected cell loss: Short-lived cells (T^*)		Long-lived cells (M^*) Confidence interval				Latently infected cells (L) Confidence interval				Proviral DNA		Steady-state values	
	CD4 cells (per μl)	HIV-1 RNA (per ml)	δ (d^{-1})	$t_{1/2}$ (d)	μ_M (d^{-1})	Lower	Upper	$t_{1/2}$ (d)	μ_L (d^{-1})	Lower	Upper	$t_{1/2}$ (d)	δ_{DNA} (d^{-1})	$t_{1/2}$ (d)	T_0^*/L_0	pM_0^*/cV_0
31	277	95,670	0.36	1.9	0.071	0.016	0.100	9.8	0.111	0.066	0.141	6.2	0.013	53	12.8	0.02
32	58	321,400	0.76	0.9	0.089	0.086	0.092	7.8	NA	NA	NA	NA	0.0016	433	NA	NA
33	505	218,800	0.74	0.9	0.036	0.023	0.052	19.3	0.055	0.028	0.077	12.6	0.025	28	26.4	0.01
37	205	42,940	1.20	0.6	0.028	0.015	0.039	24.8	0.181	0.169	0.189	3.8	0.033	21	0.5	0.04
39	216	65,520	0.51	1.4	0.034	0.030	0.039	20.4	0.088	0.073	0.101	7.9	0.0070	99	31.3	0.02
40	26	648,200	0.81	0.9	0.115	0.115	0.115	6.0	NA	NA	NA	NA	0.0024	289	NA	NA
41	321	45,840	0.58	1.2	0.037	0.031	0.043	18.7	0.049	0.036	0.060	14.1	0.0067	103	8.0	0.07
42	86	208,800	0.63	1.1	0.119	0.106	0.130	5.8	0.105	0.071	0.130	6.6	0.0052	133	16.4	0.06
Mean	212	205,896	0.70	1.1	0.066			14.1	0.098			8.5	0.012	145	15.9	0.04
s.d.	158.7	204,652	0.25	0.4	0.038			7.5	0.048			4.0	0.011	144	11.4	0.02

Baseline HIV-1 RNA values are averages of measurements taken at 3 time points over the month preceding start of therapy; baseline CD4 counts are an average of two measurements. Lower and upper 68% confidence intervals were calculated by a bootstrap method[25] in which each experiment was simulated 1,000 times. From the parameter estimates and formulae for the pretreatment quasi-steady state, values of T_0^*, L_0 and pM_0^* were obtained. At steady state, $cV_0 = pM_0^* + N\delta T_0^*$. Thus, pM_0^*/cV_0 is the fraction of virions produced by infected long-lived cells. In our analysis, the parameter c was set to $c = 3\,d^{-1}$, δ_L was equal to δ_{DNA}, V_0 and T_0 were set to their baseline values, and the remaining parameters were estimated by nonlinear least-squares regression. Patients 32 and 40 were only analysed using the long-lived cell model. For patient 40, a jackknife fit was done and the most outlying data point ignored. As patient 32 was not in steady state before treatment, the data were fitted to a model in which the coefficients A and C in equation (1) were chosen as arbitrary constants rather than as functions of the steady-state parameters. NA, not applicable.

may be released into the circulation, thus serving as an additional source of viral particles during the second phase. Here, what we have termed long-lived, virus-producing cells could be interpreted to include a tissue compartment releasing virions into plasma with a rate constant p, while decaying with a net rate constant μ_M.

Our results provide evidence that the productively infected cells in blood are representative of the total body population. This follows from the observation that the $t_{1/2}$ of the first phase, determined from the rate of fall of plasma virus, corresponds to the $t_{1/2}$ seen in the initial decline of PBMC infectivity (Fig. 2a). Thus, the rate of decay of productively infected cells in blood reflects the rate of decline of such cells body-wide, suggesting that the levels of infected CD4 cells in blood and tissue are proportional. This conclusion is in good agreement with recent experimental findings[22]. Further, the rapid initial fall of PBMC infectivity provides the first direct evidence for the rapid decay of productively infected cells, previously inferred from plasma virus decay kinetics[3].

Our results have direct implications for the possibility of eradicating HIV-1 from an infected person. If *de novo* infection is completely inhibited by antiretroviral agents, the treatment duration necessary to permit all viral compartments to burn out would depend on the decay $t_{1/2}$ and pool size of each element. Given their rapid kinetics, even as many as 10^{12} pre-existing cell-free virions or 10^{12} productively infected $CD4^+$ T cells would be eliminated in less than two months. In this study, we found that the $t_{1/2}$ of infected long-lived cells ranged from about 1 to 4 weeks (Table 1); the $t_{1/2}$ of lymphocytes latently infected with infectious provirus ranged from about 1/2 to 2 weeks. The pool sizes of these two populations probably could not exceed 10^{12} cells, the total number of lymphocytes in an average person[23], or $1–3 \times 10^{11}$, the total number of macrophages[24]. Available experimental data suggest that in general the pool sizes for M^* and L are $\leq 10^9$ and 10^8 to 10^9, respectively[7,13,16–20]. Calculations based on the above estimates (Table 2) suggest that these known compartments of virus could be completely eliminated after 2.3–3.1 years of treatment with a 100%-inhibitory antiretroviral regimen. However, to eradicate HIV-1 completely from an infected person, treatment may need to be administered for a longer period, because of the possible existence of small, undetected viral compartments that decay more slowly than the second phase, or sanctuary sites (such as the brain) which are impenetrable by some or all of the antiretroviral drugs. In addition, as can be deduced from the slow decay shown in Fig. 2b, the viral DNA within mononuclear cells that could not be experimentally activated to produce infectious virus will still be present for many years and perhaps for life, leaving open a remote chance that infectious progeny could be produced. These concerns must be properly addressed in future studies. In addition, given the high cost and toxicity of prolonged combination therapy, new strategies must be developed to facilitate the extinction of those viral 'embers' that could rekindle the infection. Although significant progress has been made in the past year in the treatment of HIV-1-infection, it would be wrong to believe that we are close to a cure for AIDS. However, the recent advances in treatment and pathogenesis do warrant a close examination of the feasibility of eradicating HIV-1 from an infected person. □

Received 7 January; accepted 7 April 1997.

1. Wei, X. *et al.* Viral dynamics in human immunodeficiency virus type 1 infection. *Nature* **273,** 117–122 (1995).
2. Ho, D. D. *et al.* Rapid turnover of plasma virions and CD4 lymphocytes in HIV-1 infection. *Nature* **373,** 123–126 (1995).
3. Perelson, A. S. *et al.* HIV-1 dynamics *in vivo*: virion clearance rate, infected cell life-span, and viral generation time. *Science* **271,** 1582–1586 (1996).
4. Patick, A. K. *et al.* Antiviral and resistance studies of AG1343, an orally bioavailable inhibitor of human immunodeficiency virus protease. *Antimicrob. Agents Chemother.* **40,** 292–297 (1996).
5. Heath, S. L. *et al.* Follicular dendritic cells and human immunodeficiency virus infectivity. *Nature* **377,** 740–744 (1995).
6. Pope, M. *et al.* Conjugates of dendritic cells and memory T lymphocytes from skin facilitate productive infection with HIV-1. *Cell* **78,** 389–398 (1994).
7. Haase, A. T. *et al.* Quantitative image analysis of HIV-1 infection in lymphoid tissue. *Science* **274,** 985–989 (1996).
8. Herz, A. V. *et al.* Viral dynamics *in vivo*: limitations on estimates of intracellular delay and virus decay. *Proc. Natl Acad. Sci. USA* **93,** 7247–7251 (1996).
9. Ho, D. D., Moudgil, T. & Alam, M. Quantitation of human immunodeficiency virus type 1 in the blood of infected persons. *N. Engl. J. Med.* **321,** 1621–1625 (1989).
10. Connor, R. I., Mohri, H., Cao, Y. & Ho, D. D. Increased viral burden and cytopathicity correlate temporally with CD4+ T-lymphocyte decline and clinical progression in human immunodeficiency virus type 1-infected individuals. *J. Virol.* **67,** 1772–1777 (1993).
11. Fazekas de St Groth, S. The evaluation of limiting dilution assays. *J. Immunol. Meth.* **49,** R11–R23 (1982).
12. Nowak, M. A., Bonhoeffer, S., Shaw, G. M. & May, R. M. Antiviral drug treatment: dynamics of resistance in free virus and infected cell populations. *J. Theor. Biol.* **184,** 203–217 (1997).
13. Vesanen, M. *et al.* Stability in controlling viral replication identifies long-term nonprogressors as a distinct subgroup among human immunodeficiency virus type 1-infected persons. *J. Virol.* **70,** 9035–9040 (1996).
14. Mitchie, C. A. *et al.* Lifespan of human lymphocyte subsets defined by CD45 isoforms. *Nature* **360,** 264–265 (1992).
15. Shaw, G. M. Viral and cellular dynamics in HIV-1 infection. *Dixième Colloque des Cent Gardes* (eds Girard, M. & Dodet, B.) 9–11 (Elsevier, New York, 1995).
16. Chun, T.-W. *et al. In vivo* fate of HIV-1-infected T cells: quantitative analysis of the transition to stable latency. *Nature Med.* **1,** 1284–1290 (1995).
17. Moreno, P. *et al.* Alveolar macrophages are not an important source of viral production in HIV-1 infected patients. *AIDS* **10,** 682–684 (1996).
18. Koenig,. S. *et al.* Detection of AIDS virus in macrophages in brain tissue from AIDS patients with encephalopathy. *Science* **233,** 1089–1093 (1986).
19. Cao, Y. *et al.* Identification and quantitation of HIV-1 in the liver of patients with AIDS. *AIDS* **6,** 65–70 (1992).
20. Ho, D. D., Rota, T. R., Hirsch, M. S. Infection of monocyte-macrophages by human T lymphotropic virus type III. *J. Clin. Invest.* **77,** 1712–1715 (1986).
21. Gartner, S. *et al.* The role of mononuclear phagocytes in HTLV-II/LAV infection. *Science* **233,** 215–219 (1986).
22. Chun, T.-W. *et al.* Quantification of latent tissue reservoirs and total body viral load in HIV-1 infection. *Nature* **387,** 183–188 (1997).
23. Trepel, F. Number and distribution of lymphocytes in man. A critical analysis. *Klin. Wschr.* **52,** 511–515 (1974).
24. van Furth, R. *Inflammation: Basic Principles and Clinical Correlates* (eds Gallin, J. I., Goldstein, I. M. & Snyderman, S.) 325–339 (Raven, New York, 1992).
25. Efron, B. & Tibshirani, R. Bootstrap measures for standard errors, confidence intervals, and other measures of statistical accuracy. *Stat. Sci.* **1,** 54–77 (1986).

Acknowledgements. We thank the patients for their participation, Agouron Pharmaceutical for supporting the clinical trial, D. Chernoff and colleagues at Chiron for technical assistance, C. Macken for help in analysing the limiting dilution data, and B. Goldstein and B. Sulzer for the use of their nonlinear least-squares fitting package. Part of this work was performed under the auspices of the US Department of Energy. This work was supported by the Rockefeller University General Clinical Research Center, the Aaron Diamond Foundation, the Santa Fe Institute, the Joseph P. Sullivan and Jeanne M. Sullivan Foundation, and by grants from the NIH.

Correspondence and requests for materials should be addressed to D.D.H.

Segmental regulation of *Hoxb-3* by *kreisler*

Miguel Manzanares*, Sabine Cordes†‡, Chung-Tin Kwan§, Mai Har Sham§, Greg S. Barsh† & Robb Krumlauf*

** Division of Developmental Neurobiology, MRC National Institute for Medical Research, The Ridgeway, Mill Hill, London NW7 1AA, UK*
† Departments of Pediatrics and Genetics, and the Howard Hughes Medical Institute, Beckman Center for Molecular and Genetic Medicine, Stanford University Medical Center, Stanford, California 94305-5428, USA
§ Department of Biochemistry, The University of Hong Kong, 5 Sassoon Road, Hong Kong

***Hox* genes control regional identity during segmentation of the vertebrate hindbrain into rhombomeres[1–3]. Here we use transgenic analysis to investigate the upstream mechanisms for regulation of *Hoxb-3* in rhombomere(r)5. We identified enhancers from the mouse and chick genes sufficient for r5-restricted expression. Sequence comparisons revealed two blocks of similarity (of 19 and 45 base pairs), which each contain *in vitro* binding sites for the *kreisler* protein (Kmrl1), a Maf/b-Zip protein expressed in r5 and r6 (ref. 4). Both sites are required for r5 activity, suggesting that *Hoxb-3* is a direct target of *kreisler*. Multimers of the 19-base-pair (bp) block recreate a Krml1-like pattern in r5/r6, but the 45-bp block mediates expression only in r5. Therefore elements within the 45-bp block restrict the response to Krml1. We identified additional sequences that contain an Ets-related activation site, required for both the activation and restriction to r5. These studies demonstrate that *Krml1* directly activates expression of**

‡ Present address: Samuel Lunenfeld Research Institute, Mount Sinai Hospital, 600 University Avenue, Toronto, Ontario M5G 1XS Canada.